The Magnetic Susceptibility of the Transition Elements

C. J. KRIESSMAN, *Eckert-Mauchly Division, Remington Rand, Inc., Philadelphia, Pennsylvania*

AND

HERBERT B. CALLEN,* *Department of Physics, University of Pennsylvania, Philadelphia, Pennsylvania*

(Received October 30, 1953; revised manuscript received February 1, 1954)

The available data on the temperature dependence of the paramagnetic susceptibility of the transition elements are reviewed. A theoretical treatment according to the band theory of solids is developed explicitly by means of a simple approximation to the Fermi function. Each term in the resulting theoretical formula may be directly and graphically interpreted in terms of the geometry of the density-of-states curve, allowing a simple and intuitive analysis of the susceptibility variation at any temperature. The empirical data on the temperature coefficient of susceptibility, on the absolute magnitude of the susceptibility, and on the specific heats of the transition elements are analyzed to suggest probable alterations in the available theoretical density-of-states curves.

1. INTRODUCTION

ONLY in recent years have enough reliable data been accumulated to encourage an attempt at a general understanding of the temperature dependence of the magnetic susceptibility of the transition elements. These data,[1–16] together with the absolute magnitudes of the susceptibility and of the electronic specific heat, provide some of the most direct information on the electronic density-of-states curves of these materials.

The purpose of this paper is two-fold: first, to critically assemble the data on the temperature variation of the magnetic susceptibility, and to show that certain striking regularities in these data can be understood on the basis of the general features of the available theoretical density-of-states curves;[17] and second, to invert the logic and to suggest certain alterations in the details of the density-of-states curves on the basis of the experimental data.

The theoretical treatment which we shall develop for the temperature dependence of the susceptibility is based on a simple approximation to the Fermi function which avoids the intractable integrals of the precise theory. This approximation yields closed-form expressions valid for any temperature, and permits a simple and intuitive graphical interpretation on the basis of the density-of-states curve.

The theory supplements an earlier theory of Stoner[18] which proceeded by a series expansion valid for low temperatures. On the basis of that theory Stoner recognized the general aspects of the relationship between the density-of-states curve and the temperature dependence of the susceptibility. The geometrical nature of our analysis allows a particularly perspicuous and convenient semiquantitative discussion of recent extensive experimental data and of the various theoretical density-of-states curves.

2. EXPERIMENTAL OBSERVATIONS

The most striking feature of the accumulated data on the temperature dependence of the susceptibility of the transition elements is that each of the elements in a particular column of the periodic table exhibits the

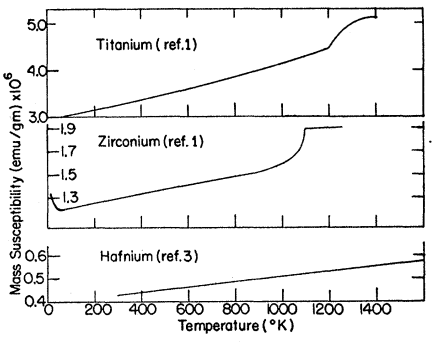

FIG. 1. Experimental susceptibilities of Ti, Zr, and Hf. The high-temperature changes in the susceptibilities of Ti and Zr are associated with crystal structure transitions.

* The contribution of one of the authors (H. B. C.) to this work was supported in part by the U. S. Office of Naval Research at the University of Pennsylvania, and was stimulated and initiated in the course of consultantship to the Eckert-Mauchly Division of Remington Rand, Inc.

[1] C. F. Squire and A. R. Kaufmann, J. Chem. Phys. **9**, 673 (1941).
[2] Li Klemm, Z. Electrochem. **45**, 354 (1939).
[3] C. J. Kriessman and T. R. McGuire, Phys. Rev. **90**, 374 (1953).
[4] C. J. Kriessman, Revs. Modern Phys. **25**, 122 (1953).
[5] F. E. Hoare and J. C. Walling, Proc. Phys. Soc. (London) **B64**, 337 (1951).
[6] W. J. deHaas and P. M. Van Alphen, Proc. Acad. Sci. Amsterdam **36**, 263 (1933).
[7] T. R. McGuire and C. J. Kriessman, Phys. Rev. **85**, 452 (1952).
[8] L. F. Bates and A. Baqui, Proc. Phys. Soc. (London) **B48**, 781 (1936).
[9] H. Söchtig, Ann. Physik **38**, 97 (1940).
[10] M. Isobe, Science Repts. Tôhoku Univ. **A3**, 78 (1951).
[11] A. Serres, J. phys. radium **9**, 377 (1938).
[12] N. Perakis and L. Capatos, Compt. rend. **196**, 611 (1933).
[13] A. N. Guthrie and L. T. Bourland, Phys. Rev. **37**, 303 (1931).
[14] K. Honda, Ann. Phys. **32**, 1027 (1910).
[15] F. E. Hoare and J. C. Mathews, Proc. Roy. Soc. (London) **A212**, 137 (1952).
[16] For a compilation of electronic specific heat data see M. Horowitz and J. G. Daunt, Phys. Rev. **91**, 1099 (1953).
[17] H. M. Krutter, Phys. Rev. **48**, 664 (1935); J. C. Slater, Phys. Rev. **49**, 537 (1936).
[18] E. C. Stoner, Proc. Roy. Soc. (London) **A154**, 656 (1936).

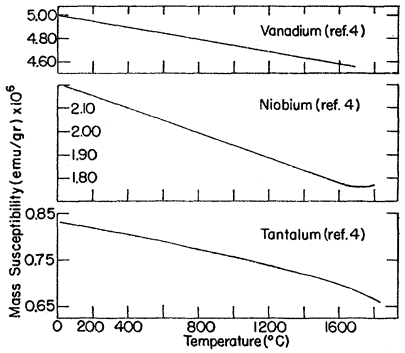

FIG. 2. Experimental susceptibilities of V, Nb, and Ta.

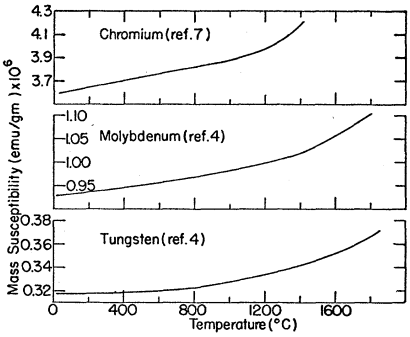

FIG. 3. Experimental susceptibilities of Cr, Mo, and W.

same general type of temperature dependence; thus the susceptibility of each of the elements (Ti, Zr, Hf) in column IV increases with increasing temperature, whereas the susceptibility of each of the elements (V, Nb, Ta) in column V decreases with increasing temperature. Furthermore, the sign of the temperature coefficient of the susceptibility is observed to alternate from column to column of the periodic table. The empirical results are shown in a series of graphs, (Figs. 1–6), references to which are given in Table I. Since many of the room temperature values of the absolute magnitude of the susceptibility which are quoted in handbooks are antiquated, a list of the best values has been compiled in Table II. It should be noted that only a room temperature value is known for Re, and that the data on Ru, Os, and Ir are still somewhat uncertain.

TABLE I. References and figures for the experimental magnetic susceptibility data.

Periodic table column	Elements	References	Dominant temperature dependence	Figure
IV	Ti;Zr;Hf	1,2;1,2;3	increasing	1
V	V;Nb;Ta	4,2;4,6;4,5	decreasing	2
VI	Cr;Mo;W	7,8,9;4,6;4,6	increasing	3
VII	Mn;Re	11,3,10;12	decreasing	4
VIII	Ru;Os	13;13,14	increasing	5
IX	Rh;Ir	5,15,13;13,14	increasing	6;5
X	Pd;Pt	5,13,15;13,15	decreasing	6

As remarked above, one of the most interesting features of the experimental data is that the temperature coefficient of the susceptibility alternates in sign with the columns in the periodic table from column IV to column VIII. This change in temperature coefficient correlates also with an alternation in the magnitudes of both the room temperature susceptibility and the electronic specific heat[16] as shown in Table III. These facts will be discussed in the following section in relation to the band theory. The burden on a theory has become more difficult with the recent discovery of maxima in the susceptibilities of Mn (Fig. 4) and Pd (Fig. 6) and minima in the susceptibilities of Zr (Fig. 1) and Nb (Fig. 2). However, it must be noted that although the maxima have been substantiated, it is possible that the low-temperature minimum in Zr is due to impurities, as indicated by Squire and Kaufmann,[1] and that the apparent high-temperature minimum in Nb may be merely a leveling off. Another interesting result is that the susceptibility of Pd appears to increase again at the lowest temperatures.

3. INTERPRETATION ACCORDING TO THE BAND THEORY

We recall very briefly the mechanism of the Pauli paramagnetism. In the absence of a magnetic field the electronic spins in a paramagnetic material are equally divided between the two possible spin states ("up" and "down"). An applied magnetic field in the up direction lowers the energies of the electrons with spin up relative to those with spin down. The lowest energy state of the system is then achieved by a spontaneous transition of some electrons from the down to the up state. The net

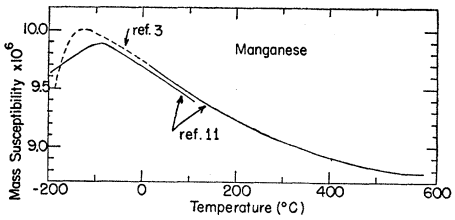

FIG. 4. Experimental susceptibility of Mn. The original dotted data are higher than shown, but have been shifted downward to join continuously with the solid curve.

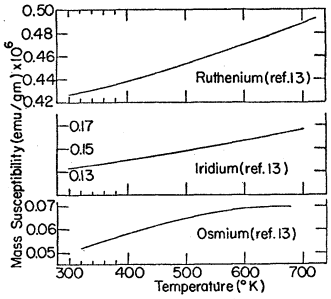

FIG. 5. Experimental susceptibilities of Ru and Os (column VIII of the periodic table) and of Ir (column IX).

uncompensated magnetic moment so induced per unit field is the magnetic susceptibility of the material.

The total number of electrons with spin up is simply $\int n_+(\epsilon)f(\epsilon,\zeta,T)d\epsilon$, where $n_+(\epsilon)$ is the density-in-energy of the electronic spin-up states; $f(\epsilon,\zeta,T)$ is the Fermi distribution function (the *a priori* probability of occupation of a state of energy ϵ); and ζ and T are the Fermi energy and absolute temperature, respectively. The applied magnetic field merely lowers the energy of every spin-up eigenstate by the amount μH, so that

$$n_+(\epsilon)=n(\epsilon+\mu H), \tag{1}$$

where $n(\epsilon)$ is the density-in-energy of the states of a single spin in the absence of a magnetic field. Similarly,

$$n_-(\epsilon)=n(\epsilon-\mu H). \tag{2}$$

The Fermi energy ζ is determined by the requirement that the sum of the numbers of electrons of each spin is the constant total number N:

$$N=\int[n(\epsilon+\mu H)+n(\epsilon-\mu H)]f(\epsilon,\zeta,T)d\epsilon. \tag{3}$$

The susceptibility is given in terms of the difference between the number of spins up and the number of spins down:

$$\chi=\operatorname*{Lim}_{H\to 0}\frac{\mu}{H}\int[n(\epsilon+\mu H)-n(\epsilon-\mu H)]f(\epsilon,\zeta,T)d\epsilon. \tag{4}$$

This equation is easily cast into a more convenient form by first explicitly performing the indicated limiting process,

$$\chi=2\mu^2\int n'(\epsilon)f(\epsilon,\zeta,T)d\epsilon, \tag{5}$$

and by then performing a partial integration,

$$\chi=-2\mu^2\int n(\epsilon)f'(\epsilon,\zeta,T)d\epsilon, \tag{6}$$

Equations (3) and (6) are the fundamental equations determining the susceptibility. In principle it would merely be necessary to know $n(\epsilon)$ from the band structure of the material; one would solve for ζ from Eq. (3), insert this into Eq. (6), and then perform the integration to obtain χ explicitly as a function of T.

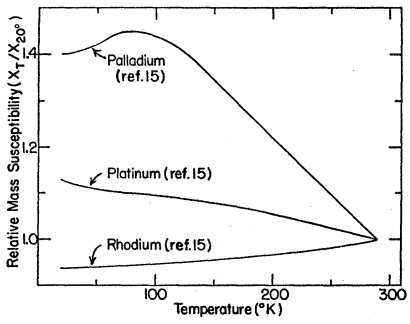

FIG. 6. Experimental susceptibilities of Rh (column IX) and of Pd and Pt (column X). The general trends of the susceptibility dependence continue in the high-temperature region which is not shown in the graph.

TABLE II. Compilation of best magnetic susceptibility values (emu/g) for the transition elements.

Element	$\chi\times10^6$	References
Ti	3.2	1,2
Zr	1.3	1,2
Hf	0.42	3
V	5.0	4
Nb	2.24	4,6
Ta	0.84	4,5
Cr	3.3	8,7
Mo	0.94	4,6
W	0.30	4,6
Mn	9.7	11
Re	0.37	12
Ru	0.43	13
Os	0.05	13
Rh	0.99	5
Ir	0.18	14,16
Pd	5.23	5
Pt	0.97	5

TABLE III. Comparison of the temperature coefficient of the susceptibility, the electronic specific heat, and the magnetic susceptibility of certain transition elements.

	Ti	V	Cr	Mn	(Ru)
Sign of $d\chi/dT$	+	−	+	−	+
Electronic specific heat, $\gamma\times10^4$	8.0	15	3.8	42	3.04
Susceptibility, $\chi\times10^6$	3.2	5.0	3.3	9.7	0.43

However, for any realistic $n(\epsilon)$ functions, this simple procedure is mathematically awkward due to the difficulty of the integrations involving $f(\epsilon,\zeta,T)$. Now although the susceptibility does depend on the Fermi distribution function (which is the same for all the metals), the main differences in the susceptibility from one metal to another will depend on the differences in their $n(\epsilon)$ curves. Since the susceptibility does not depend critically on the fine details of the universal function $f(\epsilon,\zeta,T)$, we replace it by an analytically simple function which still retains the essential character of $f(\epsilon,\zeta,T)$ and which makes the mathematical calculations relatively easy and convenient. Such a function is shown in Fig. 7 and is given algebraically by

$$f^*(\epsilon,\zeta,T)=\begin{cases}1, & \epsilon<\zeta-2.77kT\\ \frac{1}{2}\left(1-\dfrac{\epsilon-\zeta}{2.77kT}\right), & \zeta-2.77kT<\epsilon<\zeta+2.77kT\\ 0, & \epsilon>\zeta+2.77kT.\end{cases} \tag{7}$$

We now proceed to substitute this simple linearized function into our basic Eqs. (6) and (3) in order to obtain a new pair of simplified basic equations. Substituting first into Eq. (6) gives

$$\chi=-2\mu^2\int_{\zeta-2.77kT}^{\zeta+2.77kT}n(\epsilon)\left(-\frac{1}{5.5kT}\right)d\epsilon, \tag{8}$$

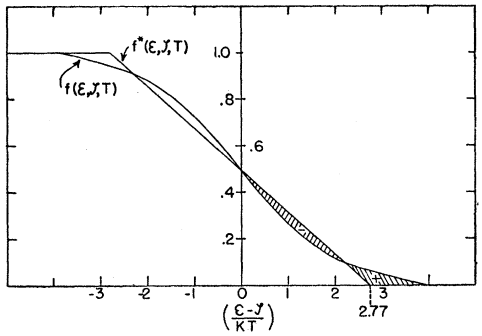

FIG. 7. The "linear" approximation to $f(\epsilon,\zeta,T)$. The slope of the straight line is so chosen that the shaded area vanishes algebraically.

or

$$\chi=2\mu^2\langle n(\zeta)\rangle_{5.5kT}. \tag{9}$$

That is, the magnetic susceptibility is proportional to the average value of $n(\epsilon)$ in an energy interval of width 5.5kT, centered at $\epsilon=\zeta$.

The simplification of Eq. (3) proceeds in a similar fashion, but the result is not quite so immediate. For the vanishingly small values of magnetic field in which we are interested Eq. (3) becomes

$$N=2\int_{-\infty}^{\infty} n(\epsilon)f(\epsilon,\zeta,T)d\epsilon. \tag{10}$$

Eliminating N by means of the above equation rewritten for $T=0$, and replacing f by the linearized function f^*, we obtain

$$\int_{\infty}^{\infty} n(\epsilon)[f^*(\epsilon,\zeta,T)-f(\epsilon,\zeta_0,0)]d\epsilon=0. \tag{11}$$

Now the first fact which may be noted is that ζ is bounded in an interval of width $5.5kT$, centered at ζ_0:

$$\zeta_0-2.77kT<\zeta<\zeta_0+2.77kT. \tag{12}$$

For if we were to assume $\zeta>\zeta_0+2.77kT$, the term in square brackets in the integrand of Eq. (11) would be everywhere nonnegative, and the integral consequently could not vanish. Similarly, if we were to assume $\zeta<\zeta_0-2.77kT$, the term in square brackets would be everywhere nonpositive and again the integral could not vanish. It is now convenient to introduce an integrated density-of-states curve defined by

$$N(\epsilon,\zeta_0)=\int_{\zeta_0}^{\epsilon} n(\epsilon')d\epsilon'. \tag{13}$$

Thus $N(\epsilon,\zeta_0)$ has the physical significance of the total number of states (of a single spin) between the energies ζ_0 and ϵ. In the counting of states, however, all states of energy higher than ζ_0 give a positive contribution, whereas all states of energy less than ζ_0 give a negative contribution. An $N(\epsilon,\zeta_0)$ curve obtained from the $n(\epsilon)$ curve computed by Slater and Krutter[17] for copper is shown in Fig. 8.

Given a particular $n(\epsilon)$ curve, construction of the $N(\epsilon,\zeta_0)$ curves for various values of ζ_0 is facilitated by the evident relation,

$$N(\epsilon,\zeta_0')=N(\epsilon,\zeta_0)-N(\zeta_0',\zeta_0). \tag{14}$$

Thus we need only compute one integrated density-of-states curve; all others can be obtained therefrom by the simple subtraction of an appropriate constant. Equation (11), which determines ζ, may now be put into a convenient form by a partial integration,

$$\int_{-\infty}^{\infty} N(\epsilon,\zeta_0)\frac{d}{d\epsilon}[f^*(\epsilon,\zeta,T)-f(\epsilon,\zeta_0,0)]d\epsilon=0; \tag{15}$$

and inserting the algebraic form for the parenthetical function yields

$$\langle N(\zeta,\zeta_0)\rangle_{5.5kT}=0. \tag{16}$$

That is, the Fermi energy is determined by the vanishing of the average value of the integrated density-of-states curve in an interval 5.5kT centered at $\epsilon=\zeta$.

Equations (9) and (16) are our new basic pair of equations, replacing (6) and (3). The procedure for computing the susceptibility at any given temperature now resolves into the following sequence of graphical constructions, which are illustrated in Fig. 9. We assume that we are given the density-of-states curve $n(\epsilon)$ and the zero-temperature Fermi energy ζ_0 (or the equivalent quantity N, the total number of electrons). We then construct the integrated density-of-states curve $N(\epsilon,\zeta_0)$. To find the value of ζ at the chosen temperature T we move the interval $5.5kT$ along the energy axis until it intercepts an algebraically vanishing area under the $N(\epsilon,\zeta_0)$ curve. The center of the interval is then $\zeta(T)$. The average value of the $n(\epsilon)$ curve in that interval, when multiplied by the constant $2\mu^2$, is the value of the susceptibility $\chi(T)$.

Although the above constructions permit a simple

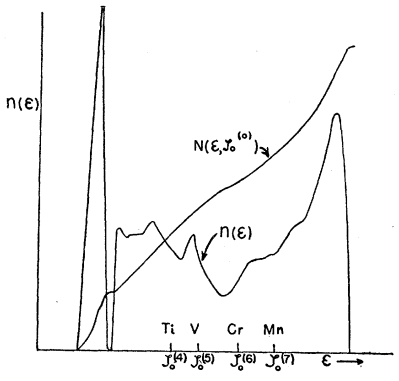

FIG. 8. The density-of-states curve for copper, as computed by Slater and Krutter. The integrated density-of-states curve $N(\epsilon,\zeta_0^{(0)})$ is also shown. The relative positions of other energies $\zeta_0^{(n)}$ for some of the transition elements are indicated (n is the total number of s and d electrons).

calculation of $\chi(T)$ itself, it is in the temperature coefficient $d\chi/dT$ that we are primarily concerned. We shall now see that this quantity may also be directly related to certain geometrical constructions based on the $n(\epsilon)$ curve.

The temperature dependence of χ clearly arises from two distinct sources. These are

1. the variation with temperature of the *width* of the Fermi distribution and consequently of the interval of averaging in Eq. (9). This width is simply $5.5kT$;
2. the variation with temperature of the Fermi energy $\zeta(T)$, which determines the *center* of the interval of averaging in Eq. (9). The dependence of ζ on the temperature is determined by Eq. (16).

The two separate mechanisms of temperature variation are clearly exhibited in the explicit equation for the derivative. Differentiating Eq. (9) (or 8), we find

$$\frac{d\chi}{dT}=\frac{2\mu^2}{T}[\bar{n}(\zeta\pm 2.77kT)-\langle n(\zeta)\rangle_{5.5kT}]$$
$$+2\mu^2\left[\frac{n(\zeta+2.77kT)-n(\zeta-2.77kT)}{5.5kT}\right]\frac{d\zeta}{dT}, \quad (17)$$

where $\bar{n}(\zeta\pm 2.77kT)$ denotes the average of the two values of $n(\epsilon)$ at the ends of the interval:

$$\bar{n}(\zeta\pm 2.77kT)=\tfrac{1}{2}[n(2.77kT)+n(\zeta+2.77kT)]. \quad (18)$$

The two terms of Eq. (17) correspond, respectively, to the two sources of temperature variation mentioned above. The quantity $d\zeta/dT$ may be related to the density-of-states curve by differentiating Eq. (16), yielding

$$\frac{d\zeta}{dT}=-2.77k\frac{N(\zeta+2.77kT,\zeta_0)+N(\zeta-2.77kT,\zeta_0)}{N(\zeta+2.77kT,\zeta-2.77kT)}. \quad (19)$$

Each of the terms of Eqs. (17) and (19) may be given a direct geometrical interpretation in terms of the $n(\epsilon)$ curve, and this geometrical interpretation is very useful in the analysis of susceptibility data. To interpret the first term of Eq. (17), which represents the contribution of the width of the Fermi distribution, we consider a straight line drawn between the values of $n(\epsilon)$ at the ends of the interval $\zeta\pm 2.77kT$. The bracket in the first term is then proportional (with the factor $5.5kT$) to the algebraic area between this line and the actual $n(\epsilon)$ curve, as shown in Fig. 9. To interpret the second term in Eq. (17), we note that the bracket is just the slope of the above mentioned straight line. The quantity $d\zeta/dT$, as given in Eq. (19), is in turn proportional (with the factor $5.5k$) to the fractional difference in the areas to the left and to the right of ζ_0 under the $n(\epsilon)$ curve in the interval $\zeta\pm 2.77kT$. This geometrical interpretation of $d\zeta/dT$ is illustrated in Fig. 9.

We shall now consider each of the two mechanisms of temperature variation in more detail. The first contribution to $d\chi/dT$, arising from the width of the Fermi distribution, is $2\mu^2/5.5kT^2$ times the area between the $n(\epsilon)$ curve and the straight line joining the extremities of the interval. It is clear that this contribution depends essentially on the curvature of $n(\epsilon)$ in the interval $\zeta\pm 2.77kT$. If $n(\epsilon)$ were linear, the curve would be coincident with the straight line, and the area between them would vanish; analytically, the average value of $n(\epsilon)$ appearing in Eq. (17) would just be $n(\zeta)$, independent of the width of the interval. However, if $n(\epsilon)$ were to have positive curvature the curve would be below the line, and the area would be positive, connoting a positive contribution to $d\chi/dT$. In terms of Eq. (9) the average value of $n(\epsilon)$ would be larger than $n(\zeta)$ and would increase with increasing interval width $5.5kT$; as a result the susceptibility would tend to increase with temperature. Similarly, an $n(\epsilon)$ curve with negative curvature leads to a negative temperature coefficient of susceptibility. This connection with the curvature is clearly evident in the first term of Eq. (17), the form of which suggests the finite difference approximation to the second derivative of $n(\epsilon)$.

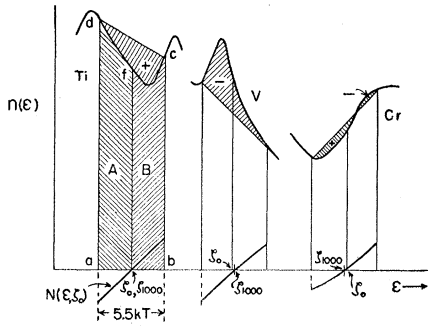

FIG. 9. Geometrical interpretation of the two contributions to the temperature coefficient of the susceptibility. Portions of the Slater-Krutter density-of-states curve have been applied to Ti, V, and Cr. The contributions of the interval width to the temperature coefficient of the susceptibility is (for Ti).

$$(d\chi/dT)_{\text{width}}=2\mu^2/5.5kT^2 \quad (\text{Area } dfc).$$

The contribution of the Fermi energy shift is

$$(d\chi/dT)_{\text{shift}}=2\mu^2(\text{slope of line } dc)(d\zeta/dT),$$

where

$$d\zeta/dT=5.5k[(\text{Area A}-\text{Area B})/(\text{Area A}+\text{Area B})].$$

For low temperatures we may expand $n(\epsilon)$ in a power series about $\epsilon=\zeta$:

$$n(\epsilon)=n(\zeta)+(\epsilon-\zeta)n'(\zeta)+(1/2!)(\epsilon-\zeta)^2n''(\zeta)+\cdots, \quad (20)$$

whence

$$\langle n(\zeta)\rangle_{5.5kT}=n(\zeta)+\frac{(2.77)^2}{2(2!)}n''(\zeta)(kT)^2+\frac{(2.77)^4}{4(4!)}n^{(iv)}(\zeta)(kT)^4+\cdots. \quad (21)$$

Again we note that the leading temperature-dependent term is determined by the curvature of $n(\epsilon)$, and we

also note that the temperature dependence involves only even powers of T.

Two significant physical conclusions thus may be drawn from these considerations. First, that the contribution to the temperature dependence of the width of the interval of averaging appears only in a quadratic, and not in a linear, term in T. And second, that the contribution of this mechanism to the temperature coefficient of χ is positive if ζ_0 lies near a minimum of $n(\epsilon)$ (where $n(\epsilon)$ is concave upward) and is negative if ζ_0 lies near a maximum of $n(\epsilon)$ (where $n(\epsilon)$ is concave downward).

We now consider the second contribution to the temperature dependence of the susceptibility, namely, the variation of the Fermi energy with temperature. If an increase in temperature shifts ζ in the direction of increasing $n(\zeta)$ this mechanism tends to make a positive contribution to the temperature coefficient of χ, whereas if an increase of T shifts ζ in the direction of decreasing $n(\zeta)$ the contribution tends to be negative. Thus the second term of Eq. (17) is roughly of the form $(dn/d\epsilon)_\zeta d\zeta/dT$, the actual slope $(dn/d\epsilon)_\zeta$ being replaced, however, by the slope of the straight line joining the values $n(\zeta\pm 2.77kT)$. The value of $d\zeta/dT$ is found graphically as described above and as indicated in Fig. 9.

It is again of some interest to check the behavior at low temperatures. Expanding $N(\epsilon,\zeta_0)$ in a power series about $\epsilon=\zeta_0$, we obtain

$$N(\epsilon,\zeta_0)=(\epsilon-\zeta_0)n(\zeta_0)+\frac{1}{2!}(\epsilon-\zeta_0)^2n'(\zeta_0)+\frac{1}{3!}(\epsilon-\zeta_0)^3n''(\zeta_0)+\cdots, \quad (22)$$

whence

$$\langle N(\zeta,\zeta_0)\rangle=(\zeta-\zeta_0)n(\zeta_0)+\frac{1}{2!}[(\zeta-\zeta_0)^2+\tfrac{1}{3}(2.77kT)^2]n'(\zeta_0)+\cdots. \quad (23)$$

By ignoring all terms higher than the second in T, the equation obtained by equating $\langle N(\zeta,\zeta_0)\rangle$ to zero may be solved for ζ, giving

$$\zeta-\zeta_0=-\frac{1}{6}\frac{n'(\zeta_0)}{n(\zeta)}(2.77kT)^2. \quad (24)$$

Thus

$$n(\zeta)=n\left(\zeta_0-\frac{1}{6}\frac{n'(\zeta_0)}{n(\zeta_0)}(2.77kT)^2\right)=n(\zeta_0)-\frac{1}{6}\frac{[n'(\zeta_0)]^2}{n(\zeta_0)}(2.77kT)^2+\cdots. \quad (25)$$

Inserting this value in Eq. (21) we find that to the second order in T,

$$\chi=2\mu^2n(\zeta_0)+(2.77)^2\mu^2\left[\tfrac{1}{2}n''(\zeta_0)-\frac{(n'(\zeta_0))^2}{3n(\zeta_0)}\right](kT)^2. \quad (26)$$

The term involving the square of the first derivative of $n(\epsilon)$ is the contribution of the variation of ζ with temperature. Again we find that the temperature dependence appears only in a quadratic, rather than in a linear, term in T. The sign of this leading temperature-dependent term is always negative, so that at low temperatures the shift of ζ with temperature always makes a negative contribution to the temperature coefficient of the susceptibility.

Equation (26) may be compared with a result of Stoner,[18] who by a direct series expansion of the true Fermi function, found

$$\chi=2\mu^2n(\zeta_0)+\frac{\pi^2}{2}\mu^2\left[\tfrac{1}{3}n''(\zeta_0)-\frac{[n'(\zeta_0)]^2}{3n(\zeta_0)}\right](kT)^2+\cdots. \quad (27)$$

On the basis of this low-temperature equation, Stoner[18] has demonstrated the possibility of obtaining a positive temperature coefficient of susceptibility near a minimum of $n(\epsilon)$, and has applied this result to a discussion of the then-available data.

Despite the fact that at very low temperatures the contribution to $d\chi/dT$ of the shift of ζ is always negative, at reasonable temperatures this contribution may be either positive or negative. The graphical solution indicates that ζ has a tendency to move away from the largest peak of the $n(\epsilon)$ curve in the interval $\zeta\pm 2.77kT$, and this "repulsion" may easily result in an increase in $n(\zeta)$ with T. A condition under which this mechanism will contribute a positive temperature coefficient is thus that ζ_0 be on the shallow side of an asymmetric minimum of $n(\epsilon)$.

4. THEORETICAL DENSITY-OF-STATES CURVES[19]

Preparatory to a discussion of the correlation of the theoretical results and the empirical data, we briefly review the several density-of-states curves which have been computed for the transition elements. Precise calculations, although possible in principle, are prohibitively difficult in practice. As a consequence semiquantitative inferences must be drawn from the synthesis of the results of various approximate calculations.

The theoretical density-of-states curve to which we shall make primary reference is that computed by Slater and Krutter[17] for copper, and generally optimistically applied to the various iron-group transition metals. The Slater-Krutter calculation is based on an approximate Wigner-Seitz solution of the Fock equations, using an ion-core potential obtained from the Hartree functions for the free copper ion. As these Hartree functions, in turn, were computed neglecting exchange they are very probably larger than the true inner-core functions. Consequently the width of the d band as computed by Krutter is undoubtedly too wide. The computed width is 5.4 ev, whereas a more probable

[19] G. V. Raynor, "The band structure of metals," Repts. Progr. Phys. 15, 173 (1952).

value on the basis of soft x-ray data, electronic specific heats, and other calculations is of the order of 4 ev.

The general method of the Slater-Krutter calculations on copper have been applied to α Fe by Manning[20] and to γ Fe by Greene and Manning.[21] Comparison of these curves with the copper curve substantiates to some extent the assumption of similarity in form of the d band among the various transition metals, although significant differences in detail are quite apparent. In all three curves the distribution is peaked at each end of the band, and has a third peak just below the center of the band. Although the relative heights of the peaks differ in the various calculations we shall see that it is merely the existence and position of the peaks, rather than their precise height, which is significant in our considerations.

Another calculation with relevance to the Fe-group transition metals is the tight-binding calculation of Ni by Fletcher and Wohlfarth.[22] The tight-binding approximation certainly underestimates the effect of overlap, and in this case predicts a band width of only 2.7 ev.

For our discussions of the density-of-states curves of the elements in the sixth row of the periodic table (Hf, Ta, W, Re, Os, Ir, Pt) we shall refer principally to the calculation of tungsten by Manning and Chodorow,[23] shown in Fig. 10. This calculation employed a rather elaborate Wigner-Seitz cellular approach, using fourteen atomic functions for the representation of the wave functions of the valence electrons. The results for the partially filled d band may be expected to be reasonably accurate, and the extrapolation of the results to Ta at least should be quite trustworthy. Extrapolation to other members of the sixth row, which have other crystal structures, would be questionable.

No theoretical density-of-states curves are available for a discussion of the transition elements of the fifth row of the periodic table (Zr, Nb, Mo, Ru, Rh, Pd).

5. THEORETICAL CORRELATION OF EXPERIMENTAL DATA

Having reviewed both the experimental data and the theory of the dependence of the susceptibility on the density-of-states curves, we now consider the correlation of the observed data with the $n(\epsilon)$ curves described in the preceding section. In particular we shall first attempt to account for the observed alteration in the sign of $d\chi/dT$ from column to column of the periodic table. The empirical susceptibility data will then be analyzed to suggest certain probable alterations in the details of the theoretical density-of-states curves.

We first consider the sequence of the iron-group transition metals, for which we adopt the Slater-Krutter curve as the nominal basis for our discussion. We proceed by assessing the separate contributions to $d\chi/dT$ from the interval width and from the ζ shift mechanisms using the graphical constructions illustrated in Fig. 9. We arbitrarily choose an interval width of 1000°C to obtain the general trend of the temperature coefficient of the susceptibility. If both mechanisms give contributions of the same algebraic sign, the sign of $d\chi/dT$ is known immediately. However, if the two separate contributions are of opposite sign we must inquire more carefully into the ratio of their magnitudes. We shall examine in turn the elements Ti, V, Cr, and Mn. In Fig. 9 we see that for Ti the motion of ζ over the temperature interval to 1000°C is very small because the areas under $N(\epsilon,\zeta_0)$ are almost equal. However, it is evident from the relative heights of the two maxima that ζ will shift slightly to the right, the direction of decreasing $n(\epsilon)$ and decreasing χ. The contribution due to the interval width, however, is positive and large. The ratio of the interval width contribution to the ζ shift contribution is of the order of 80, showing conclusively that the susceptibility of Ti should increase with temperature over 1000°C. This is in agreement with the experimental data in Fig. 1.

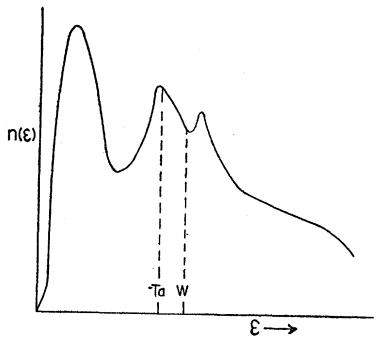

FIG. 10. The density-of-states curve for tungsten, as calculated by Manning and Chodorow. The zero-temperature Fermi energy of W and Ta are indicated.

The same constructions for V are also shown in Fig. 9 It is evident that both the interval width and ζ shift mechanisms give negative contributions to $d\chi/dT$ in this case and that as a result the susceptibility of V should decrease with temperature. Again this is consistent with the experimental data shown in Fig. 2.

Cr is considered next. From Fig. 9 we find that $(d\chi/dT)_{\text{width}}$ is positive while $(d\chi/dT)_{\zeta\text{ shift}}$ is negative. The calculated value of the ratio of these contributions is 1.06 indicating that the χ of Cr should actually increase with temperature in accord with the experimental data in Fig. 3. However, the low value of the ratio is somewhat unconvincing. Also, as Friedberg, Estermann, and Goldman[24] have pointed out, and as is evident from Table II, Cr has a much lower electronic specific heat than its neighbors in the periodic table. Since the electronic specific heat is directly proportional to $n(\epsilon)$ we would expect the Fermi energy of Cr to occur at a very

[20] M. F. Manning, Phys. Rev. **63**, 190 (1943).
[21] J. B. Greene and M. F. Manning, Phys. Rev. **63**, 203 (1943).
[22] G. C. Fletcher and E. P. Wohlfarth, Phil. Mag. **42**, 106 (1951).
[23] M. F. Manning and M. Chodorow, Phys. Rev. **56**, 787 (1939).
[24] Friedberg, Estermann, and Goldman, Phys. Rev. **85**, 375 (1952).

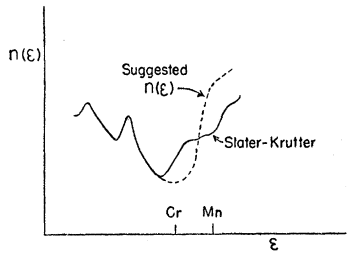

FIG. 11. The Slater-Krutter density-of-states curve qualitatively altered from considerations of the experimental susceptibility and electronic specific heat data.

low minimum in $n(\epsilon)$. This would be most logically accomplished if the minimum in $n(\epsilon)$, which in Fig. 8 occurs between V and Cr, were widened considerably. Then not only would the ζ_0 of Cr occur at a lower value of $n(\epsilon)$, but the density-of-states in the neighborhood of Mn would be increased significantly. This is physically desirable also because the magnitudes of the susceptibility and electronic specific heat of Mn are much larger than those of Cr. This suggests that the actual $n(\epsilon)$ curve is of the form shown in Fig. 11. From this curve it is at once clear that the susceptibility of Cr must increase with temperature since there will now be a larger positive interval width contribution.

The suggested $n(\epsilon)$ curve also serves to clarify the case of Mn, in which the experimental susceptibility decreases with temperature in the intermediate temperature range. The ζ_0 of Mn falls on one side of a large maximum in the $n(\epsilon)$ curve of Slater and Krutter, a position which ordinarily would lead to a negative $d\chi/dT$. However, as can be seen in Fig. 8, the fortuitous positioning of ζ_0 near what is probably only a computational secondary minimum in $n(\epsilon)$ predicts a positive $d\chi/dT$, even though ζ moves toward lower $n(\epsilon)$. Our suggested $n(\epsilon)$ curve eliminates this presumably computational minimum and gives the temperature dependence suggested by the broader features of the Slater-Krutter $n(\epsilon)$ and required by experiment.

Thus we have the important result from our simplified treatment that the band theory applied to a slightly amended approximate calculation of the $3d$ band is capable of explaining the observed alternation in sign of $d\chi/dT$ of the transition elements. This alternation arises from the sequence of maxima and minima which have appeared in roughly similar form in the various various approximate calculations of the density-in-energy curves of the iron-group $3d$ band. Corroborating evidence for the validity of maxima and minima in the density-of-states of the transition elements is found in the electronic specific heat. At low temperatures the electronic portion of the specific heat may be represented by a term linear in temperature, $C_e=\gamma T$, where γ is directly proportional to $n(\zeta)$. Goldman[25] has pointed out that the values of $n(\zeta)$ derived from the electronic specific heats of the transition elements alternate in a manner quite like the maxima and minima in the Slater-Krutter curve. Recently Horowitz and Daunt[16] have also proposed an $n(\epsilon)$ curve, somewhat similar to that of Fig. 11, based on a synthesis of the electronic specific heat data of the transition elements. It seems reasonable therefore, to state that a structure of maxima and minima in the $3d$ band is capable of explaining the susceptibilities of the Fe-group elements, and that this structure is in harmony both with theoretical calculations and with other experimental data.

The temperature dependence of the susceptibility of tungsten, in the sixth row of the periodic table, may be discussed on the basis of the density-of-states curve computed by Manning and Chodorow and shown in Fig. 10. The Fermi energy falls at a minimum as shown, and $d\chi/dT$ is consequently positive, in agreement with the experimental susceptibility shown in Fig. 3. On the basis of the same theoretical density-of-states curve the zero-temperature Fermi energy of tantalum falls at a maximum of $n(\epsilon)$, as indicated in Fig. 10. A negative coefficient of susceptibility is thereby predicted, again in agreement with the experimental observations.

Maxima and minima in the curves of susceptibility *vs* temperature present no special problem to our treatment, although in some cases it may be necessary to resort to fine structure in the $n(\epsilon)$ curves. Minima at low temperatures are easily explained. It has been pointed out that at low temperatures the movement of ζ always results in a decreasing χ; therefore, if the interval width contribution is the smaller at low temperatures (i.e., if the curvature $n''(\zeta_0)$ is small) the χ will necessarily decrease. As T increases the interval width contribution, if positive, can easily cause the sign of $d\chi/dT$ to change, thereby producing the low temperature minima. A maximum at low temperatures is somewhat more difficult to explain because of the tendency of the susceptibility to decrease at low temperatures; but if ζ_0 were to occur at a small depression in $n(\epsilon)$, the susceptibility could increase initially at low temperatures and a maximum could easily result. However, it must be pointed out that in the case of manganese a strong exchange coupling may be responsible for the maximum at low temperatures. Maxima and minima at high temperatures are easily accounted for in terms of the competition of the two mechanisms.

On the basis of the above simplified treatment, it thus appears that the band theory is able to give a natural explanation not only of the increasing χ of certain transition elements, but also of the remarkable alternation in sign of $d\chi/dT$.

[25] J. Goldman (private communication).